

Clark Amerault\* and Xiaolei Zou

The Florida State University, Tallahassee, Florida

## 1 INTRODUCTION

Accurate prediction of precipitation fields in numerical weather prediction (NWP) remains a daunting task. Mesoscale models such as the fifth-generation Penn State / National Center for Atmospheric Research Mesoscale Model (MM5, Dudhia 1993) allow for the prediction of a number of hydrometeor fields using any of a number of explicit moisture schemes. Unfortunately, it has been difficult to perform an exhaustive test on these schemes because of the lack of directly measured hydrometeor observations. Realizing that remote sensing techniques will become more and more prevalent in the validation of NWP parameterization schemes, recent studies have focused on the response of radiative transfer calculations to the parameters in explicit moisture schemes, (Bauer et al. 2000; Skofronick-Jackson et al. 2002).

Furthermore, the superensemble technique (Krishnamurti et al. 2000, Shin and Krishnamurti 2003) has been shown to greatly improve precipitation skill for global scale models. One way in which this technique can be applied is to use the same model with different physical parameterization schemes to comprise the ensemble members. The goal of this study is to apply the superensemble technique to the assimilation of satellite measured brightness temperatures ( $T_b$ s), which are sensitive to the prediction of hydrometeor fields of the MM5. Preliminary results of this study will be presented at the conference.

## 2 FORECAST MODEL AND OBSERVATIONS

### 2.1 Explicit Moisture Schemes

For the MM5 there are eight different explicit moisture scheme options, of these, only four include prediction of precipitating ice phase hydrometeors. These four schemes will be used for this study. Two schemes are based on the work of Riesner et al.

(1998, hereafter referred to as R1 and R2). The Goddard (GD) scheme is based on the work of Tao and Simpson (1989), and Schultz (SH, 1995) has also contributed a scheme. In the least, each of the four schemes contains predictive equations for the mixing ratios of cloud water  $q_c$ , cloud ice  $q_{ci}$ , rain water  $q_r$ , and snow ice  $q_{si}$ . The R2, GD, and SH schemes also predict the mixing ratio of graupel  $q_g$ , and the R2 scheme includes additional prognostic equations for the total number concentration of cloud ice  $N_i$ , snow  $N_s$ , and graupel  $N_g$ . The R1, R2, and GD schemes are based on the works of Lin et al. (1983) and Rutledge and Hobbs (1983) where the size distribution of precipitating liquid drops and ice crystals are assumed to follow an inverse exponential function

$$N_x(D) = N_{x0} \exp(-\lambda D) \quad (1)$$

and

$$\lambda = \left( \frac{\pi \rho_x N_{x0}}{\rho q_x} \right)^{0.25} \quad (2)$$

where  $N_x(D)$  is the number of drops with diameters between  $D$  and  $D+dD$  for hydrometeor class  $x$  ( $x = r$  for rain,  $x = s$  for snow, and  $x = g$  for graupel). The mixing ratio of a hydrometeor class is given by  $q_x$  and the density by  $\rho_x$ , while  $\rho$  is the density of the moist air.  $N_{x0}$  is known as the intercept parameter, and  $\lambda$  is referred to as the slope. Many of the source and sink terms in these schemes are based on the parameters in (1) and (2). On the other hand, in the SH scheme all of source/sink terms were formulated to depend on only the mixing ratio  $q_x$  or the specific content  $r_x$  (mass of condensate per unit volume) of a hydrometeor class.

In order to determine  $\lambda$  and therefore  $N(D)$ , the value of  $N_0$  must first be determined. In the R1 and GD schemes the value of  $N_0$  is a constant which has been empirically determined for all precipitating hydrometeors (rain and snow as well as graupel in the GD scheme). In the complex R2 scheme only the value of  $N_{r0}$  is constant. As mentioned above, the R2 scheme includes predictive equations for  $N_s$  and  $N_g$  as well as  $N_i$ , which means  $N_{s0}$  and  $N_{g0}$  can be diagnosed at each time step from the

\*Corresponding author address: Clark Amerault, Department of Meteorology, The Florida State University, Tallahassee, FL 32306-4520

values of  $N_s$  and  $N_g$ , respectively. Table 1 contains more information on the specifics of the explicit moisture schemes used in this study, including the values of  $N_{x0}$  and  $\rho_x$  for each class of precipitating hydrometeors.

## 2.2 Radiative Transfer Model

In order to evaluate the performance of these schemes using SSM/I  $T_b$ s the fast radiative transfer model developed by Liu (1998, RTML) is used to compute brightness temperatures from output of the MM5. Previously, the  $T_b$ s produced by the RTML at 85 GHz were as much as 100 K less than the coldest observed  $T_b$ s in areas of high model produced ice concentrations (Amerault and Zou 2003). In order to decrease this large and undesirable difference, the Maxwell-Garnett mixing formula was added to the calculation of the dielectric constant for mixtures of ice and air. After adding this formula, the value of  $\rho_s$  could be altered to lessen the difference between the lowest observed and forecasted  $T_b$  at 85 GHz. In order to make the RTML more consistent with the output from the MM5, the RTML now accepts snow ice  $q_s$  and graupel  $q_g$  as input and the values of  $N_{s/g0}$  and  $\rho_{s/g}$  have been changed to reflect the values of the explicit moisture schemes which were used to create the input of the RTML. The values of  $N_{s0}$ ,  $N_{g0}$ ,  $\rho_s$ , and  $\rho_g$  are  $0.08 \text{ cm}^{-4}$ ,  $0.04 \text{ cm}^{-4}$ ,  $0.1 \text{ g cm}^{-3}$ , and  $0.4 \text{ g cm}^{-3}$ , respectively, for the R1 scheme. For the GD scheme the values of  $N_{s0}$ ,  $N_{g0}$ ,  $\rho_s$ , and  $\rho_g$  are  $0.08 \text{ cm}^{-4}$ ,  $0.04 \text{ cm}^{-4}$ ,  $0.1 \text{ g cm}^{-3}$ , and  $0.4 \text{ g cm}^{-3}$ , respectively. The values of these parameters for the R2 and SH schemes are the same as the values for the R1 scheme.

Figure 1 shows the 85V (85 GHz vertically polarized channel)  $T_b$ s produced from output of a 36 hr MM5 forecast (6 km horizontal grid spacing) of Hurricane Bonnie using the GD scheme as well as the SSM/I observations from the same channel at approximately the same time (0000 UTC 25 August 1998). The MM5 was initialized using the Bogus Data Assimilation scheme (Zou and Xiao 2000). Although the position of the lowest  $T_b$ s (indicating areas of microwave scattering by ice particles in large convective cells) do not coincide in the forecast and observations, the magnitudes of the lowest  $T_b$ s are in much better agreement than in the results of Amerault and Zou (2003). The difference between the lowest  $T_b$ s in the forecast and observations is roughly 20 K, which gives us confidence that the updated RTML is an adequate tool to evaluate the performance of explicit moisture schemes.

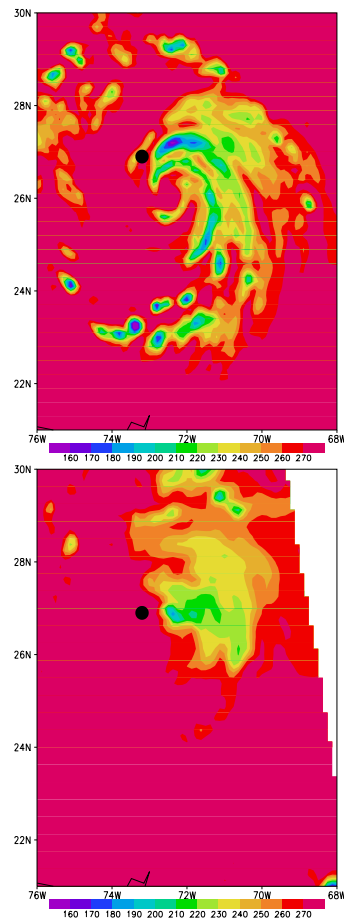


Figure 1: 85V  $T_b$ s produced by the RTML from a 36 hr MM5 forecast using the GD scheme valid 0000 UTC 25 August 1998 (top), and observed 85V SSM/I  $T_b$ s from roughly the same time (bottom).  $T_b$ s are in units of K. The filled circle indicates the observed center of Hurricane Bonnie at the forecast time.

## 2.3 Experiments

Forecasts for Hurricane Bonnie were produced starting from three different time periods, 1200 UTC 23, 0000 UTC 24, and 1200 24 UTC August 1998. During this time the lowest observed central sea level pressure associated with Bonnie was 954 mb, and the highest observed winds were estimated to be 100 kts. The BDA procedure outlined in Park and Zou (2003) was used to initialize the MM5 on a domain with 18 km horizontal grid spacing. The results of the BDA procedure were then transferred to a domain with 6 km grid spacing using bilinear interpolation. For each time period eight total forecasts were run, four (one for each explicit moisture scheme) on the 6 km domain, and four more on the same domain

Table 1: Information on the explicit moisture schemes used in this study.

	R1	R2	GD	SH
Contain predictive equations for:	$q_c, q_r, q_i, q_s$	$q_c, q_r, q_i, q_s, q_g$ $N_i, N_s, N_g$	$q_c, q_r, q_i, q_s, q_g$	$q_c, q_r, q_i, q_s, q_g$
$N_{r0}$ ( $\text{cm}^{-4}$ )	0.08	0.08	0.08	NA
$N_{s0}$ ( $\text{cm}^{-4}$ )	0.08 or 0.2	Varies	0.03	NA
$N_{g0}$ ( $\text{cm}^{-4}$ )	0.04	Varies	0.0004	NA
$\rho_r$ ( $\text{g cm}^{-3}$ )	1.0	1.0	1.0	NA
$\rho_s$ ( $\text{g cm}^{-3}$ )	0.1	0.1	0.1	NA
$\rho_g$ ( $\text{g cm}^{-3}$ )	0.4	0.4	0.913	NA

with nested forecast run on a smaller domain with 2 km horizontal grid spacing. The size of the 6 km domain was 175x205 points in the horizontal with 27 vertical layers. The 2 km domains were placed near the center of the hurricane and had sizes of 151x151 points in the horizontal with 27 vertical layers. The forecasts on the 6 km domain were run for 24 hours, while the 2 km forecast only ran for the last 6 hours of the forecast time period (hours 18-24). No cumulus parameterization was used in the forecasts. All forecasts were run using the distributed memory version of the MM5 on an IBM SP3 at Florida State University.

### 3 RESULTS

The MM5 output for each of the 24 hr forecasts was used to produce  $T_b$ s with the RTML in order to compare the forecast results with the SSM/I observations. The  $T_b$ s calculated on the 6 km domain along with the observations were then interpolated using bilinear interpolation onto a domain with the same horizontal grid spacing which was comparable to the horizontal resolution of the observations. For the 85 GHz  $T_b$ s, the horizontal domain spacing was 18 km, and for all other channels it was set to 56 km. The relative frequency of the 85V  $T_b$ s for the three forecast time periods, 1200 UTC 24, 0000 UTC 25, and 1200 UTC 25 August 1998, produced by output from each of the four explicit moisture schemes on the 6 km domain without the 2 km nest, along with the relative frequency of the observations from the closest time period for each of the three forecasts are shown in Figure 2. Overall, the shape of the curves for the model data for each of the explicit moisture schemes are similar and close to the observations. They all contain peaks in the 270-280 K range, although the peaks for the SH and GD scheme are considerably higher than the peaks of the R1 and R2 curves. For the colder  $T_b$  ranges ( $< 270$  K)

the relative frequencies of the model produced  $T_b$ s is consistently higher than the observations. In these regions, the colder  $T_b$ s are indicative of precipitating ice which scatters microwave radiation and lowers the  $T_b$ , meaning each of the schemes may be producing ice over too much of the domain. Figure 3 is similar to Figure 2 except that the data from the 6 km domains with the 2 km nests were used to produce the relative frequencies of the model data. There are slight differences between the two figures, but overall, the results for the two types of forecasts for each of the explicit moisture schemes were very similar when interpolated to a grid with a larger horizontal grid spacing. For the other channels not shown, the results were similar in that each of the schemes produced relative frequencies that were close to one another as well as the observations, and the differences between the results from the 6 km domain without the 2 km nest and the 6 km domain with the 2 km nest were small.

However, this is not to say that there are not differences between the different schemes and also between nested and non-nested forecasts. Even though the previous results focused on an area encompassing a hurricane, there were still many precipitation free areas in the domain, as is evident by the large peak in the 85V  $T_b$ s at warmer temperatures. This can mask the variability between the schemes which is occurring in areas of precipitation. Figure 4 shows the relative frequencies of the  $T_b$ s produced from each of the four explicit moisture schemes from the three forecasts over the area of the 2 km nested domain. The relative frequencies are shown for the 6 km domain with the 2 km nest and without it, as well from data from the 2 km nest. No interpolation was performed on the data. The 2 km nest was placed near the center of the hurricane so that areas of intense convection and precipitation would be included in the results. In this area of heavy precipi-

tation, not only are there major differences between the explicit moisture schemes, but also between the different domain configurations. The 2 km and 6 km with the 2 km nest results are similar because of the feedback between the two domains during the forecast. The relative frequencies from the 6 km domain without the nest are noticeably different than the other two domains especially for the GD, R2, and SH schemes. The shapes of the curves between the schemes are also much different. All schemes show a secondary peak in relative frequency in the 280-290 K range indicating areas where there was no precipitating ice; however, the primary peaks vary from scheme to scheme. For the R1 and R2 schemes, the primary peak is located in the 220-240 K range, depending on the domain configurations, while for the GD scheme the primary peak is in the 250-265 K range. The SH scheme curve is relatively broad with a peak around 210 K for the nested results, and more peaked toward 270 K for the 6 km domain without the nest. The relative frequency plots for the other channels (not shown) show similar patterns as in the 85V data, which is that there is variability in the  $T_b$ s produced both by the different schemes and by the different domain configurations.

#### 4 FUTURE WORK

Now that we have seen that there are differences between the different explicit moisture schemes and different grid spacing configurations, we hope to conduct data assimilation experiments using an ensemble set of forecasted  $T_b$ s in the minimization of a cost function involving the difference between the observed  $T_b$ s and the ensemble forecast  $T_b$ s. The ensemble forecasted  $T_b$  will result from a weighted average of  $T_b$ s calculated by the RTML from output of the different explicit moisture schemes discussed above. To determine the weights we will conduct data assimilation experiments using SSM/I observations to produce a best guess estimate for the actual observed hydrometeor field. This will be done by a variational procedure which will produce the hydrometeor field which results in a  $T_b$  closest to the observations. The challenge to this procedure is producing an appropriate background field of hydrometeor values in order to make it a well posed problem. Without the background field, the procedure would have to produce on the order of a 150 values (5 different hydrometeor variables at 30 levels) from only 7 observations (one  $T_b$  each of the SSM/I channels). The background field will likely be composed of averages of the hydrometeor fields from the forecasts already performed and placed in rain or no rain categories. Once the best guess estimate

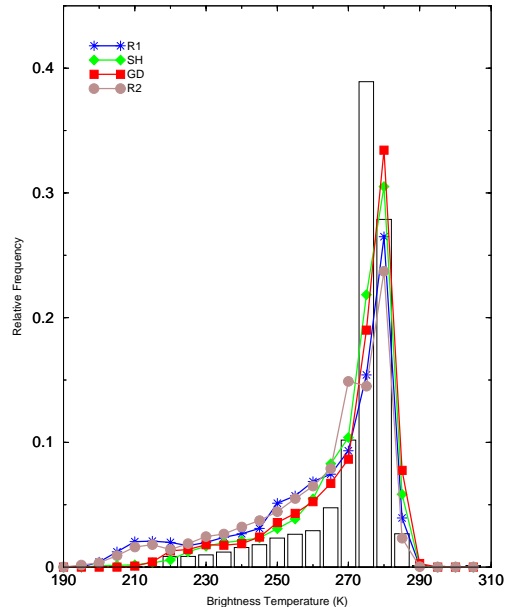


Figure 2: Relative frequency (5 K bins) of 85V  $T_b$ s interpolated to a domain with 18 km horizontal grid spacing. The  $T_b$ s produced from the R1 (blue), R2 (brown), SH (green), and GD (red) schemes from three 24 hour forecasts on a domain with 6 km grid spacing of Hurricane Bonnie valid at 1200 UTC 24, 0000 UTC 25, and 12000 UTC August 1998 were used. SSM/I observations from the nearest time period are binned. Only points where both an observed and model forecasted  $T_b$  were used.

of the hydrometeor fields is obtained, then a linear regression will be performed on a number of different profiles using data from each of the schemes to determine weights for each of the schemes. Preliminary results of this effort will be given at the conference

#### 5 ACKNOWLEDGMENTS

This work was funded by the Office of Naval Research under grants N0014-99-1-0022 and N-0014-01-0375. The authors would like to thank Dr. Guosheng Liu for providing the codes for the RTML and ways to improve the performance, and also Mr. Jeff Hawkins for providing the SSM/I observations used in this study.

#### 6 REFERENCES

- Amerault, C., X. Zou, 2003: Preliminary steps in assimilating SSM/I brightness temperatures in a hurricane prediction scheme. *J. Ocean. Atmos. Tech.*, **20**, 1154-1169.

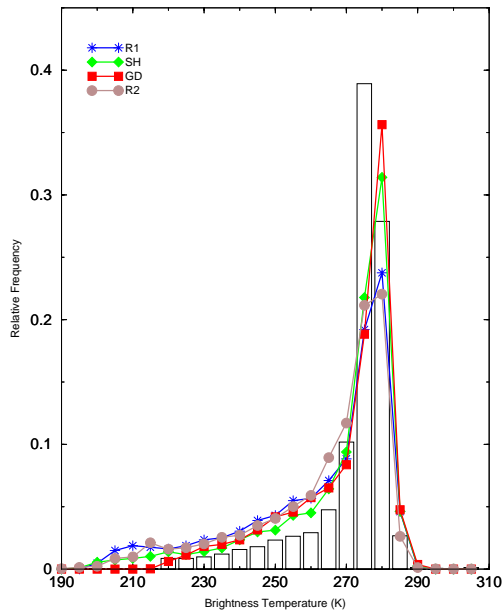


Figure 3: Same as Figure 2 except the model forecasted  $T_b$ s were taken from forecasts on the 6 km domain with a 2 km domain nested near the center of the hurricane for the last 6 hours of the forecast period.

- Bauer, P., A. Khain, A. Pokrovsky, R. Meneghini, C. Kummerow, F. Marzano, and J. Baptista, 2000: Combined cloud-microwave radiative transfer modeling of stratiform rain. *J. Atmos. Sci.*, **57**, 182-1104.
- Dudhia, J., 1993: A nonhydrostatic version of the Penn State-NCAR Mesoscale Model: Validation tests and simulation of an Atlantic cyclone and cold front. *Mon. Wea. Rev.*, **121**, 1493-1513.
- Krishnamurti, T., C. Kishtawal, D. Shin, and C. Williford, 2000: Improving tropical precipitation forecasts from a multianalysis. *J. Clim.*, **45**, 4217-4227.
- Lin, Y.-L., R. Farley, and H. Orville, 1983: Bulk parameterization of the snow field in a cloud model. *J. Clim. App. Met.*, **22**, 1065-1092.
- Liu, G., 1998: A fast and accurate model for microwave radiance calculations. *J. Met. Soc. Jap.*, **76**, 335-343.
- Park, K., and X. Zou, 2003: Toward developing an objective 4D-Var BDA scheme for hurricane initialization based on TPC observed parameters. Submitted to *Mon. Wea. Rev.*.
- Reisner, J., R. Rasmussen, and R. Brientjes, 1998: Explicit forecasting of supercooled liquid wa-

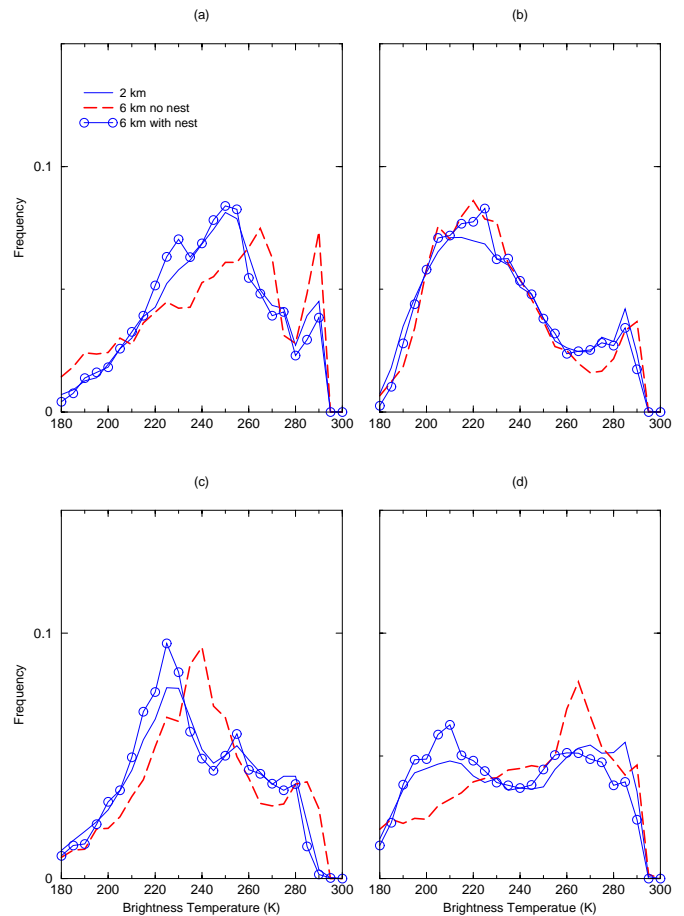


Figure 4: Relative frequency (5 K bins) of the 85V  $T_b$ s over the area of the 2 km nested domain produced by the (a) GD scheme, (b) R1 scheme, (c) R2 scheme, and (d) the SH scheme. No interpolation was performed on the 2 km (blue), 6 km with the 2 km nest (blue with open circles), or 6 km without a nest (red) results.  $T_b$ s were calculated from three 24 hr forecasts valid at 1200 UTC 24, 0000 UTC 25, and 12000 UTC August 1998.

ter in winter storms using the MM5 mesoscale model. *Q. J. R. Meteorol. Soc.*, **124**, 1071-1107.

Rutledge, S. and P. Hobbs, 1983: The mesoscale and microscale structure and organization of clouds and precipitation in midlatitude cyclones, VIII: A model for the “seeder-feeder” process in warm-frontal rainbands. *J. Atmos. Sci.*, **40**, 1185-1206.

Schultz, P., 1995: An explicit cloud physics parameterization for operational numerical weather prediction. *Mon. Wea. Rev.*, **123**, 3331-3343.

- Shin, D., and T. Krishnamurti, Short- to medium-range superensemble precipitation forecasts using satellite products: 1. Deterministic forecasting. *J. Geophys. Res.*, **108(D8)**, 8383.
- Skofronick-Jackson, G., A. Gasiewski, and J. Wang, 2002: Influence of microphysical cloud parameterizations on microwave brightness temperatures. *IEEE. Trans. Geo. Rem. Sens.*, **40**, 187-196.
- Tao W.-K., and J. Simpson, 1989: A further study of cumulus interaction and mergers: Three-dimensional simulations with trajectory analyses. *J. Atmos. Sci.*, **46**, 2974-3004.
- Zou, X., and Q. Xiao, 2000: Studies on the initialization and simulation of a mature hurricane using a variational bogus data assimilation scheme. *J. Atmos. Sci.*, **57**, 836-860.